NRC Research Press

ARTICLE

POCOP-type cobalt and nickel pincer complexes bearing an appended phosphinite group

Yingze Li, Jeanette A. Krause, and Hairong Guan

Abstract: The reaction of 1,3,5-(^{i}Pr$_2$PO)$_3$C$_6$H$_3$ with Co$_2$(CO)$_8$ leads to the isolation of a POCOP-type mononuclear pincer complex {κ^P,κ^C,κ^P-2,4,6-(^{i}Pr$_2$PO)$_3$C$_6$H$_2$}Co(CO)$_2$ (**1**) or a tetranuclear species {κ^P-{κ^P,κ^C,κ^P-2,4,6-(^{i}Pr$_2$PO)$_3$C$_6$H$_2$}Co(CO)$_2$}$_2$Co$_2$(CO)$_6$ (**2**), depending on the ligand to cobalt ratio employed. The latter compound can be an impurity during the synthesis of {2,6-(^{i}Pr$_2$PO)$_2$-4-Me$_2$N-C$_6$H$_2$}Co(CO)$_2$, when the ligand precursor 5-(dimethylamino)resorcinol is contaminated with phloroglucinol due to incomplete monoamination. Similarly, the reaction of 1,3,5-(^{i}Pr$_2$PO)$_3$C$_6$H$_3$ with NiCl$_2$ in the presence of 4-dimethylaminopyridine provides {κ^P,κ^C,κ^P-2,4,6-(^{i}Pr$_2$PO)$_3$C$_6$H$_2$}NiCl (**3**) bearing an appended phosphinite group. Structures **1–3** have been studied by X-ray crystallography.

Key words: phosphinite, pincer complexes, C–H activation, appended functionality, catalyst immobilization.

Résumé : La réaction du 1,3,5-(^{i}Pr$_2$PO)$_3$C$_6$H$_3$ avec le Co$_2$(CO)$_8$ permet d'isoler le complexe de ligand pince mononucléaire de type POCOP {κ^P,κ^C,κ^P-2,4,6-(^{i}Pr$_2$PO)$_3$C$_6$H$_2$}Co(CO)$_2$ (**1**) ou l'espèce tétranucléaire {κ^P-{κ^P,κ^C,κ^P-2,4,6-(^{i}Pr$_2$PO)$_3$C$_6$H$_2$}Co(CO)$_2$}$_2$Co$_2$(CO)$_6$ (**2**), selon le rapport ligand-cobalt utilisé. Cette dernière espèce peut être une impureté issue de la synthèse du {2,6-(^{i}Pr$_2$PO)$_2$-4-Me$_2$N-C$_6$H$_2$}Co(CO)$_2$, lorsque le précurseur de ligand 5-(diméthylamino)résorcinol est contaminé par du phloroglucinol en raison d'une monoamination incomplète. De manière similaire, la réaction du 1,3,5-(^{i}Pr$_2$PO)$_3$C$_6$H$_3$ avec le NiCl$_2$ en présence de 4-diméthylaminopyridine produit le {κ^P,κ^C,κ^P-2,4,6-(^{i}Pr$_2$PO)$_3$C$_6$H$_2$}NiCl (**3**) portant un groupe phosphinite attaché. Nous avons étudié les structures **1–3** par radiocristallographie. [Traduit par la Rédaction]

Mots-clés : phosphinite, complexes de ligands pinces, activation de liaison C–H, groupe fonctionnel attaché, immobilisation du catalyseur.

Introduction

Diphosphinite-derived POCOP-type pincer complexes have been studied extensively as homogeneous catalysts for a wide variety of organic transformations.[1–11] To facilitate catalyst–product separation and catalyst recycling,[12,13] Lewis basic functional groups can be strategically built into the pincer backbone to allow the catalysts to be immobilized on a solid support. One particularly effective functionality is an additional, free phosphinite group, which has been shown to anchor the POCOP-pincer unit on γ-alumina,[14–16] silica,[15,16] or hydrotalcite-derived Mg(Al)O[16] through the release of a secondary phosphine oxide (Scheme 1*a*). Given that many phosphinites undergo facile cyclometalation with metals such as palladium and rhodium,[7] we hypothesize that phosphinite-appended POCOP-type pincer complexes also could serve as precursors to some interesting heterobimetallic compounds (Scheme 1*b*).

We came across this specific class of POCOP-type pincer complexes in our recent study of cobalt complexes with the formulas {2,6-(^{i}Pr$_2$PO)$_2$-4-R′-C$_6$H$_2$}Co(CO)$_2$ (R′ = H, NMe$_2$, OMe, CO$_2$Me).[17] Synthesis of these pincer complexes was straightforward except for the *N*,*N*-dimethylamino derivative (δ_P = 227.87 ppm, in C$_6$D$_6$), which was frequently contaminated with an impurity displaying phosphorus resonances at 230.30 and 214.80 ppm. This problem can, however, be solved if the ligand precursor 5-(dimethylamino) resorcinol is rigorously purified.[18] We thus suspected that the impurity originated from incomplete monoamination of phloroglucinol with dimethylamine (Scheme 2).[19,20] The unreacted phloroglucinol would then be converted to triphosphinite 1,3,5-(^{i}Pr$_2$PO)$_3$C$_6$H$_3$, which in turn might also participate in the C–H activation process with Co$_2$(CO)$_8$. In this work, we test this hypothesis by first studying the reaction of 1,3,5-(^{i}Pr$_2$PO)$_3$C$_6$H$_3$ with Co$_2$(CO)$_8$ in greater detail. In addition to identifying the structure of the impurity that plagued our previous synthesis, we demonstrate C–H activation as a viable strategy to make phosphinite-appended POCOP-type pincer complexes of both cobalt and nickel.

Materials and methods

General methods

Unless otherwise noted, all organometallic compounds were prepared and handled under an argon atmosphere using standard glovebox and Schlenk techniques. Dry and oxygen-free THF, toluene, and pentane were collected from an Innovative Technology solvent purification system and used throughout the experiments. Methanol was degassed by bubbling argon through it for 30 min and then dried over 4 Å molecular sieves. Dichloromethane-d_2 (99.5% D) was purchased from Cambridge Isotope Laboratories, Inc., and used without further purification. Benzene-d_6 (99.5% D) was dried over sodium–benzophenone and distilled under an argon atmosphere. Chemical shift values for ^{1}H and ^{13}C{^{1}H} NMR spectra were referenced internally to the residual solvent resonances. ^{31}P{^{1}H} NMR spectra were referenced externally to

Received 2 April 2020. Accepted 5 May 2020.

Y. Li, J.A. Krause, and H. Guan. Department of Chemistry, University of Cincinnati, Cincinnati, OH 45221-0172, USA.
Corresponding author: Hairong Guan (email: hairong.guan@uc.edu).

This paper is part of a special issue to honour Professor Robert H. Morris.

Scheme 1. Benefits or potential benefits of developing phosphinite-appended POCOP-type pincer complexes: (*a*) catalyst immobilization; (*b*) precursors to heterobimetallic compounds.

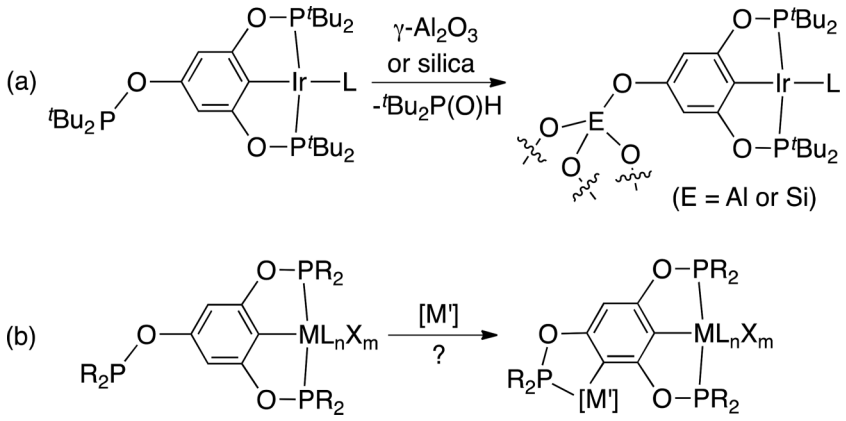

Scheme 2. Impurity potentially arising from incomplete monoamination of phloroglucinol.

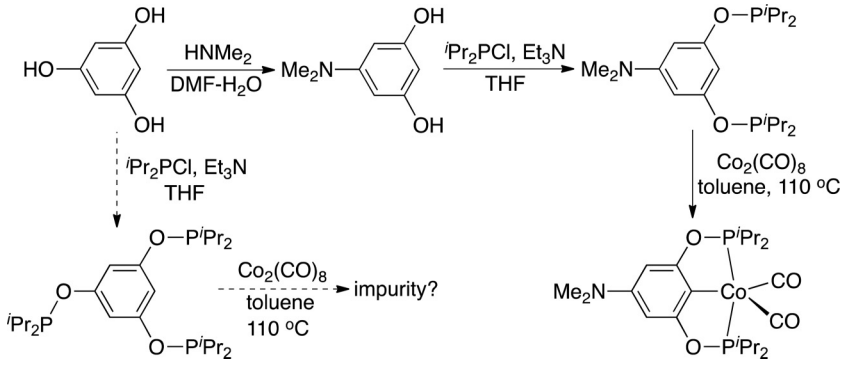

85% H_3PO_4 (0 ppm). Infrared spectra were recorded on a PerkinElmer Spectrum Two FTIR spectrometer equipped with a smart orbit diamond attenuated total reflectance (ATR) accessory.

Synthesis of 1,3,5-(^{i}Pr$_2$PO)$_3$C$_6$H$_3$

To a Schlenk flask containing a well-stirred mixture of phloroglucinol (2.00 g, 15.9 mmol), Et_3N (7.74 mL, 55.5 mmol), and THF (50 mL) was added a solution of ^{i}Pr$_2$PCl (8.33 mL, 52.3 mmol) in THF (20 mL). The mixture was stirred at room temperature for 24 h, at which point a voluminous amount of white precipitate formed. The volatiles were removed under reduced pressure, resulting in a yellow oily residue, which was extracted with pentane (3 × 60 mL) and filtered into another Schlenk flask via a cannula. The combined pentane filtrates were concentrated under vacuum to afford the product as a yellow oil (7.44 g, 99% yield, ~95% purity). This ligand was used for the subsequent syntheses without further purification. ^{1}H NMR (400 MHz, C_6D_6, δ): 6.93–6.92 (m, Ar*H*, 3H), 1.73 (sept of d, $J_{H\text{-}H}$ = 7.2 Hz, $J_{P\text{-}H}$ = 2.8 Hz, PC*H*(CH$_3$)$_2$, 6H), 1.08 (dd, $J_{P\text{-}H}$ = 10.6 Hz, $J_{H\text{-}H}$ = 7.2 Hz, PCH(C*H*$_3$)$_2$, 18H), 0.96 (dd, $J_{P\text{-}H}$ = 16.0 Hz, $J_{H\text{-}H}$ = 7.2 Hz, PCH(C*H*$_3$)$_2$, 18H). ^{13}C{^{1}H} NMR (101 MHz, C_6D_6, δ): 161.54 (d, $J_{P\text{-}C}$ = 9.6 Hz, ^{i}Pr$_2$PO*C*), 103.07 (t, $J_{P\text{-}C}$ = 11.5 Hz, Ar*C*), 28.60 (d, $J_{P\text{-}C}$ = 18.6 Hz, P*C*H(CH$_3$)$_2$), 17.88 (d, $J_{P\text{-}C}$ = 20.7 Hz, PCH(*C*H$_3$)$_2$), 17.16 (d, $J_{P\text{-}C}$ = 8.6 Hz, PCH(*C*H$_3$)$_2$). ^{31}P{^{1}H} NMR (162 MHz, C_6D_6, δ): 147.91 (s).

Synthesis of {κ^P,κ^C,κ^P-2,4,6-(^{i}Pr$_2$PO)$_3$C$_6$H$_2$}Co(CO)$_2$ (1)

To a Schlenk flask containing a solution of $Co_2(CO)_8$ (0.30 g, 0.88 mmol) in toluene (15 mL) was added a solution of 1,3,5-(^{i}Pr$_2$PO)$_3$C$_6$H$_3$ (1.25 g, 2.63 mmol) in toluene (20 mL). The flask was heated in a 110 °C oil bath for 24 h, during which time the colour of the reaction mixture changed gradually from dark red to orange–yellow. The volatiles were removed under vacuum. The resulting yellow semisolid was treated with 40 mL of pentane and filtered into another Schlenk flask via a cannula. The filtrate was concentrated under vacuum to give a yellow oily residue, which was triturated with chilled methanol (0 °C, 3 × 1.5 mL). After drying under vacuum, the desired product was isolated as a yellow solid (0.48 g, 46% yield). ^{1}H NMR (400 MHz, C_6D_6, δ): 6.86 (d, $J_{P\text{-}H}$ = 1.6 Hz, Ar*H*, 2H), 2.28–2.16 (m, coordinated PC*H*(CH$_3$)$_2$, 4H), 1.71 (sept of d, $J_{H\text{-}H}$ = 7.2 Hz, $J_{P\text{-}H}$ = 2.4 Hz, free PC*H*(CH$_3$)$_2$, 2H), 1.18–1.06 (m, PCH(C*H*$_3$)$_2$, 30H), 0.94 (dd, $J_{P\text{-}H}$ = 15.6 Hz, $J_{H\text{-}H}$ = 7.2 Hz, free PCH(C*H*$_3$)$_2$, 6H). ^{1}H NMR (400 MHz, CD_2Cl_2, δ): 6.23 (s, Ar*H*, 2H), 2.57–2.42 (m, coordinated PC*H*(CH$_3$)$_2$, 4H), 1.87 (sept, $J_{H\text{-}H}$ = 6.8 Hz, free PC*H*(CH$_3$)$_2$, 2H), 1.33–1.20 (m, coordinated PCH(C*H*$_3$)$_2$, 24H), 1.15 (dd, $J_{P\text{-}H}$ = 10.4 Hz, $J_{H\text{-}H}$ = 6.8 Hz, free PCH(C*H*$_3$)$_2$, 6H), 1.08 (dd, $J_{P\text{-}H}$ = 15.6 Hz, $J_{H\text{-}H}$ = 7.2 Hz, free PCH(C*H*$_3$)$_2$, 6H). ^{13}C{^{1}H} NMR (101 MHz, C_6D_6, δ): 205.80 (t, $J_{P\text{-}C}$ = 14.0 Hz, *C*O), 165.37 (t, $J_{P\text{-}C}$ = 8.0 Hz, Ar*C*$_{ortho}$), 159.05 (d, $J_{P\text{-}C}$ = 9.4 Hz, Ar*C*$_{para}$), 96.50 (dt, $J_{P\text{-}C}$ = 10.4 and 6.9 Hz, Ar*C*$_{meta}$), 32.45 (t, $J_{P\text{-}C}$ = 13.0 Hz, coordinated PCH(CH$_3$)$_2$), 28.64 (d, $J_{P\text{-}C}$ = 18.6 Hz, free P*C*H(CH$_3$)$_2$), 17.94 (d, $J_{P\text{-}C}$ = 20.7 Hz, free PCH(*C*H$_3$)$_2$), 17.26 (d, $J_{P\text{-}C}$ = 8.8 Hz, free PCH(*C*H$_3$)$_2$), 16.90 (t, $J_{P\text{-}C}$ = 1.5 Hz, coordinated PCH(*C*H$_3$)$_2$), 16.75 (s, coordinated PCH(*C*H$_3$)$_2$). ^{13}C{^{1}H} NMR (101 MHz, CD_2Cl_2, δ): 205.50 (t, $J_{P\text{-}C}$ = 12.2 Hz, *C*O), 164.88 (t, $J_{P\text{-}C}$ = 8.0 Hz, Ar*C*$_{ortho}$), 158.45 (d, $J_{P\text{-}C}$ = 9.1 Hz, Ar*C*$_{para}$), 128.46 (t, $J_{P\text{-}C}$ = 22.3 Hz, Ar*C*$_{ipso}$), 96.21 (dt, $J_{P\text{-}C}$ = 9.3 and 6.8 Hz, Ar*C*$_{meta}$), 32.67 (t, $J_{P\text{-}C}$ = 13.0 Hz, coordinated PCH(CH$_3$)$_2$), 28.73 (d, $J_{P\text{-}C}$ = 18.1 Hz, free P*C*H(CH$_3$)$_2$), 18.03 (d, $J_{P\text{-}C}$ = 20.3 Hz, free PCH(*C*H$_3$)$_2$), 17.30 (d, $J_{P\text{-}C}$ = 8.9 Hz, free PCH(*C*H$_3$)$_2$), 17.08 (t, $J_{P\text{-}C}$ = 2.0 Hz, coordinated PCH(*C*H$_3$)$_2$), 16.91 (s, coordinated PCH(*C*H$_3$)$_2$). ^{31}P{^{1}H} NMR (162 MHz, C_6D_6, δ): 229.42 (s, coordinated *P*CH(CH$_3$)$_2$, 2P), 148.35 (s, free *P*CH(CH$_3$)$_2$, 1P). ^{31}P{^{1}H} NMR (162 MHz, CD_2Cl_2, δ): 229.46 (s, coordinated *P*CH(CH$_3$)$_2$, 2P), 151.00 (s, free *P*CH(CH$_3$)$_2$, 1P). Selected ATR–IR data (solid, cm^{-1}): 1969 (s, ν_{CO}), 1912 (s, ν_{CO}). Anal. Calcd for $C_{26}H_{44}O_5P_3Co$: C, 53.07; H, 7.54. Found: C, 52.80; H, 7.60.

Table 1. Crystal and refinement parameters for structures **1–3**.

Crystal	**1**	**2**	**3**
Empirical formula	$C_{26}H_{44}O_5P_3Co$	$C_{58}H_{88}O_{16}P_6Co_4$	$C_{24}H_{44}O_3P_3ClNi$
Formula mass	588.45	1462.82	567.66
Color, habit	Yellow, block	Orange, plate	Yellow, plate
Crystal dimensions (mm)	0.165 × 0.125 × 0.105	0.050 × 0.040 × 0.005	0.289 × 0.215 × 0.028
Crystal system	Triclinic	Monoclinic	Monoclinic
Space group	*P*-1	$P2_1/c$	$P2_1/c$
Z	4	2	4
a (Å)	14.4387(6)	21.8621(17)	7.5830(5)
b (Å)	14.5274(6)	12.5561(10)	10.8926(7)
c (Å)	16.1953(7)	12.8739(10)	35.657(2)
α (°)	63.633(1)	90	90
β (°)	79.801(1)	102.421(2)	95.227(2)
γ (°)	84.614(1)	90	90
Collection ranges	$-19 \le h \le 19$, $-19 \le k \le 19$, $-21 \le l \le 21$	$-29 \le h \le 29$, $-16 \le k \le 16$, $-17 \le l \le 17$	$-8 \le h \le 8$, $0 \le k \le 12$, $0 \le l \le 41$
Temperature (K)	150(2)	150(2)	150(2)
Volume (Å^3)	2995.1(2)	3451.2(5)	2932.9(3)
D_{calcd} (Mg m^{-3})	1.305	1.408	1.286
Radiation	Mo Kα; λ = 0.71073 Å	Synchrotron; λ = 0.7749 Å	Cu Kα; λ = 1.54178 Å
Absorption coefficient (μ) (mm^{-1})	0.765	1.441	3.510
Absorption correction	Multi-scan	Multi-scan	Numerical
F(000)	1248	1524	1208
θ range for data collection (°)	1.420 to 28.372	2.052 to 31.373	2.489 to 65.065
Observed reflections	89140	44894	8610
Independent reflections	14974	8675	8610
R_{int}	0.0655	0.0553	N/A
Data/restraints/parameters	14974/0/655	8675/142/488	8610/0/302
Goodness of fit on F^2	1.016	1.020	1.213
Final *R* indices [$I > 2\sigma(I)$]	R_1 = 0.0424, wR_2 = 0.0945	R_1 = 0.0455, wR_2 = 0.1037	R_1 = 0.1061, wR_2 = 0.2852
R indices (all data)	R_1 = 0.0676, wR_2 = 0.1067	R_1 = 0.0699, wR_2 = 0.1163	R_1 = 0.1155, wR_2 = 0.2958
Largest diff. peak and hole (e Å^{-3})	0.705 and −0.292	0.760 and −0.934	0.856 and −0.722

Synthesis of {κ^P-{κ^P,κ^C,κ^P-2,4,6-(^{i}Pr$_2$PO)$_3$C$_6$H$_2$}Co(CO)$_2$}$_2$Co$_2$(CO)$_6$ (2)

To a Schlenk flask containing a solution of $Co_2(CO)_8$ (0.50 g, 1.46 mmol) in toluene (15 mL) was added a solution of 1,3,5-(^{i}Pr$_2$PO)$_3$C$_6$H$_3$ (0.69 g, 1.46 mmol) in toluene (20 mL). The flask was heated in a 110 °C oil bath for 24 h. The volatiles were removed under vacuum, giving a dark green oil, which was washed with pentane (3 × 5 mL) followed by chilled methanol (0 °C, 3 × 1.5 mL). After drying under vacuum, the product was isolated as an orange solid (0.25 g, 23% yield). ^{1}H NMR (400 MHz, C_6D_6, δ): 6.65 (s, Ar*H*, 4H), 2.35–2.18 (m, PC*H*(CH$_3$)$_2$, 12H), 1.35–0.91 (m, PCH(C*H*$_3$)$_2$, 72H). ^{1}H NMR (400 MHz, CD_2Cl_2, δ): 6.18 (br, Ar*H*, 4H), 2.76–2.19 (m, PC*H*(CH$_3$)$_2$, 12H), 1.48–0.89 (m, PCH(C*H*$_3$)$_2$, 72H). ^{13}C{^{1}H} NMR (101 MHz, C_6D_6, δ): 205.62 (t, $J_{P\text{-}C}$ = 14.6 Hz, *C*O), 203.19 (t, $J_{P\text{-}C}$ = 9.6 Hz, *C*O), 165.16 (t, $J_{P\text{-}C}$ = 7.6 Hz, Ar*C*$_{ortho}$), 151.95 (s, Ar*C*$_{para}$), 132.74 (t, $J_{P\text{-}C}$ = 21.7 Hz, Ar*C*$_{ipso}$), 100.04 (t, $J_{P\text{-}C}$ = 6.1 Hz, Ar*C*$_{meta}$), 34.40–34.15 (m, PCH(CH$_3$)$_2$), 32.50 (t, $J_{P\text{-}C}$ = 13.1 Hz, PCH(CH$_3$)$_2$), 17.71 (s, PCH(*C*H$_3$)$_2$), 17.52 (s, PCH(*C*H$_3$)$_2$), 16.84 (s, PCH(*C*H$_3$)$_2$), 16.72 (s, PCH(*C*H$_3$)$_2$). ^{13}C{^{1}H} NMR (101 MHz, CD_2Cl_2, δ): 205.32 (t, $J_{P\text{-}C}$ = 13.7 Hz, *C*O), 202.76 (t, $J_{P\text{-}C}$ = 6.7 Hz, *C*O), 164.75 (t, $J_{P\text{-}C}$ = 6.6 Hz, Ar*C*$_{ortho}$), 151.44 (s, Ar*C*$_{para}$), 132.71 (t, $J_{P\text{-}C}$ = 22.3 Hz, Ar*C*$_{ipso}$), 99.53 (br, Ar*C*$_{meta}$), 34.44–34.19 (m, P*C*H(CH$_3$)$_2$), 32.62 (t, $J_{P\text{-}C}$ = 12.6 Hz, P*C*H(CH$_3$)$_2$), 17.88 (s, PCH(*C*H$_3$)$_2$), 17.73 (s, PCH(*C*H$_3$)$_2$), 16.94 (s, PCH(*C*H$_3$)$_2$), 16.76 (s, PCH(*C*H$_3$)$_2$). ^{31}P{^{1}H} NMR (162 MHz, C_6D_6, δ): 230.30 (s, pincer *P*CH(CH$_3$)$_2$, 4P), 214.80 (s, non-pincer *P*CH(CH$_3$)$_2$, 2P). ^{31}P{^{1}H} NMR (162 MHz, CD_2Cl_2, δ): 230.15 (s, pincer *P*CH(CH$_3$)$_2$, 4P), 214.41 (s, non-pincer *P*CH(CH$_3$)$_2$, 2P). Selected ATR-IR data (solid, cm^{-1}): 1973 (m, ν_{CO}), 1956 (s, ν_{CO}), 1926 (s, ν_{CO}). Anal. Calcd for $C_{58}H_{88}O_{16}P_6Co_4$: C, 47.62; H, 6.06. Found: C, 47.68; H, 6.25.

Synthesis of {κ^P,κ^C,κ^P-2,4,6-(^{i}Pr$_2$PO)$_3$C$_6$H$_2$}NiCl (3)

To a Schlenk flask containing a mixture of $NiCl_2$ (0.30 g, 2.3 mmol), 4-dimethylaminopyridine (0.50 g, 4.1 mmol), and THF (20 mL) was added a solution of 1,3,5-(^{i}Pr$_2$PO)$_3$C$_6$H$_3$ (1.19 g, 2.5 mmol) in THF (20 mL). The reaction mixture was heated at 60 °C for 36 h. The volatiles were then removed under vacuum, giving an orange solid, which was extracted with pentane (2 × 20 mL) and filtered into another Schlenk flask. The pentane extracts were placed under vacuum until no solvent was left. The resulting solid was washed with cold methanol (0 °C, 2 × 20 mL) and dried under vacuum. The desired product was isolated as a yellow powder (0.67 g, 51% yield). ^{1}H NMR (400 MHz, C_6D_6, δ): 6.77 (d, $J_{P\text{-}H}$ = 1.6 Hz, Ar*H*, 2H), 2.25–2.11 (m, coordinated PC*H*(CH$_3$)$_2$, 4H), 1.68 (sept of d, $J_{H\text{-}H}$ = 6.8 Hz, $J_{P\text{-}H}$ = 2.4 Hz, free PC*H*(CH$_3$)$_2$, 2H), 1.43–1.32 (m, coordinated PCH(C*H*$_3$)$_2$, 12H), 1.21–1.12 (m, coordinated PCH(C*H*$_3$)$_2$, 12H), 1.06 (dd, $J_{P\text{-}H}$ = 10.6 Hz, $J_{H\text{-}H}$ = 7.0 Hz, free PCH(C*H*$_3$)$_2$, 6H), 0.90 (dd, $J_{P\text{-}H}$ = 15.8 Hz, $J_{H\text{-}H}$ = 7.4 Hz, free PCH(C*H*$_3$)$_2$, 6H). ^{13}C{^{1}H} NMR (101 MHz, C_6D_6, δ): 169.43 (t, $J_{P\text{-}C}$ = 10.6 Hz, Ar*C*$_{ortho}$), 161.92 (d, $J_{P\text{-}C}$ = 9.6 Hz, Ar*C*$_{para}$), 117.55 (t, $J_{P\text{-}C}$ = 22.5 Hz, Ar*C*$_{ipso}$), 97.24 (dt, $J_{P\text{-}C}$ = 11.1 and 6.3 Hz, Ar*C*$_{meta}$), 28.57 (d, $J_{P\text{-}C}$ = 18.5 Hz, free P*C*H(CH$_3$)$_2$), 28.08 (t, $J_{P\text{-}C}$ = 10.8 Hz, coordinated P*C*H(CH$_3$)$_2$), 17.82 (d, $J_{P\text{-}C}$ = 20.6 Hz, free PCH(*C*H$_3$)$_2$), 17.60 (t, $J_{P\text{-}C}$ = 2.7 Hz, coordinated PCH(*C*H$_3$)$_2$), 17.17 (d, $J_{P\text{-}C}$ = 8.8 Hz, free PCH(*C*H$_3$)$_2$), 16.79 (s, coordinated PCH(*C*H$_3$)$_2$). ^{31}P{^{1}H} NMR (162 MHz, C_6D_6, δ): 187.28 (s, coordinated *P*CH(CH$_3$)$_2$, 2P), 148.90 (s, free *P*CH(CH$_3$)$_2$, 1P). Anal. Calcd for $C_{24}H_{44}O_3P_3ClNi$: C, 50.78; H, 7.81. Found: C, 50.90; H, 7.97.

X-ray crystallography

Single crystals of **1**, **2**, and **3** were grown from pentane, THF–pentane, and pentane, respectively. Crystal data collection and refinement parameters are summarized in Table 1. Intensity data for **1** were collected at 150 K on a Bruker APEX-II CCD diffractometer using graphite-monochromated Mo Kα radiation, λ = 0.71073 Å. Intensity data for **2** were collected at 150 K on a Bruker PHOTON100 CMOS detector at Beamline 11.3.1 at the Advanced Light Source (Lawrence Berkeley National Laboratory) using synchrotron radiation tuned to λ = 0.7749 Å. Intensity data for **3** were collected at 150 K on a Bruker Photon-II diffractometer using a Cu microfocus X-ray source, λ = 1.54178 Å. The data frames were collected and processed using the APEX/SAINT suite of programs.

Scheme 3. Reaction of $Co_2(CO)_8$ with 3 equiv. of 1,3,5-(^{i}Pr$_2$PO)$_3$C$_6$H$_3$.

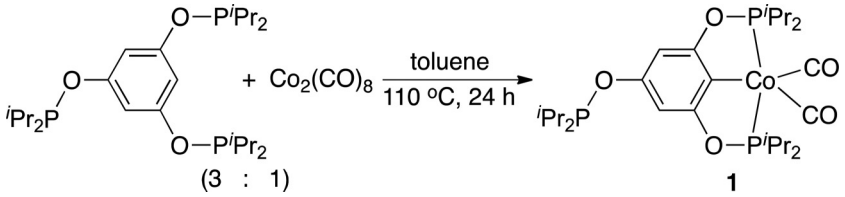

The data were corrected for decay, Lorentz, and polarization effects, as well as absorption and beam corrections, using SADABS. The structures were solved by a combination of direct methods and the difference Fourier technique and refined by full-matrix least squares on F^2 using the SHELX suite of programs. Data for **3** refines as a twin (~37%) [179.5° about the reciprocal *c* axis; twin law applied: –1.00 –0.006 0.00 0.011 –1.00 –0.001 0.845 0.001 1.00 (Cell_Now)]. Non-hydrogen atoms were refined with anisotropic displacement parameters. H-atoms were calculated and treated with a riding model. The lattices of all three complexes are devoid of solvent. Two independent molecules of **1** were found in the unit cell. For structure **2**, carbonyl groups attached to Co1 are disordered and were refined with a two-component disorder model (major component occupancy 68%). A bond distance restraint (DFIX) was applied to the Co1–C23B bond distance. The isopropyl groups attached to P2 are also disordered and refined with a two-component disorder model (major component occupancies 54% and 70% for C13 and C16 groups, respectively). Restraints were applied to the C13A–C15A/C13B–C15B and C16A–C18A/C16–C18B groups (SAME and SIMU). The crystal structures for **1–3** have been deposited at the Cambridge Crystallographic Data Centre (CCDC) and allocated the deposition numbers CCDC 1994013–1994015.

Results and discussion

The triphosphinite 1,3,5-(^{i}Pr$_2$PO)$_3$C$_6$H$_3$ needed for this study was prepared in an almost quantitative yield from phloroglucinol, chlorodiisopropylphosphine, and triethylamine mixed in THF. This ligand was isolated as a yellow oil with ~95% purity (estimated by ^{31}P{^{1}H} NMR spectroscopy) and used without further purification. The characteristic ^{13}C{^{1}H} NMR resonances (for a sample in C$_6$D$_6$) include a doublet at 161.54 ppm ($J_{P\text{-}C}$ = 9.6 Hz) and a triplet at 103.07 ppm ($J_{P\text{-}C}$ = 11.5 Hz) for the C1/C3/C5 and C2/C4/C6 carbons, respectively. The ^{31}P{^{1}H} NMR spectrum displays a singlet at 147.91 ppm, indicative of a free phosphinite ligand bearing two isopropyl groups as the *P* substituents.[21–29]

The reaction of 1,3,5-(^{i}Pr$_2$PO)$_3$C$_6$H$_3$ with $Co_2(CO)_8$ was initially carried out in a 3:1 ratio, following a similar procedure established for the synthesis of {2,6-(^{i}Pr$_2$PO)$_2$-4-R′-C$_6$H$_2$}Co(CO)$_2$ (Scheme 3).[17] The isolated yellow solid was characterized as a new cobalt dicarbonyl complex featuring two strong IR bands at 1969 and 1912 cm^{-1} attributable to CO stretches. The success of C–H activation was evident from the loss of one aromatic hydrogen, as confirmed by ^{1}H NMR spectroscopy. The ^{31}P{^{1}H} NMR spectrum of this complex **1** in C$_6$D$_6$ revealed a broad resonance at 229.42 ppm[30] and a sharp resonance at 148.35 ppm (integrated to a 2:1 ratio), consistent with the structure proposed in Scheme 3. These chemical shift values, however, do not match with those for the impurity described in the Introduction.

From a saturated pentane solution, **1** crystallizes as two independent molecules, which differ primarily in the orientation of the dangling phosphinite group (Fig. 1). Key structural parameters including the geometry index τ,[31] as summarized in Table 2, indicate that the geometry about cobalt is best described as distorted square pyramidal. The Co–C bond formed by the basal CO (i.e., C22–O22) is 0.04–0.06 Å shorter than the bond formed by the apical CO (i.e., C23–O23). The basal C–O bond is only marginally longer than the apical C–O bond. These structural features are very similar to those of {2,6-(^{i}Pr$_2$PO)$_2$-4-R′-C$_6$H$_2$}Co(CO)$_2$ studied previously by us.[17] The uniqueness of **1** is the presence of a free phosphinite group, whose P–O bond is evidently 0.02–0.03 Å longer than those as part of the POCOP pincer framework.

The reaction illustrated in Scheme 3 may not replicate the circumstance under which {2,6-(^{i}Pr$_2$PO)$_2$-4-Me$_2$N-C$_6$H$_2$}Co(CO)$_2$ was prepared, where the unintentionally made 1,3,5-(^{i}Pr$_2$PO)$_3$C$_6$H$_3$ would be overwhelmed by $Co_2(CO)_8$. Furthermore, the phosphorus chemical shifts appearing at 230.30 and 214.80 ppm imply that, for the "impurity molecule", the appended phosphinite group also binds to cobalt. These analyses prompted us to further study the reaction between 1,3,5-(^{i}Pr$_2$PO)$_3$C$_6$H$_3$ and $Co_2(CO)_8$ but using a lower ligand to cobalt ratio. Indeed, refluxing the equimolar mixture of the two in toluene led to the isolation of another cobalt complex **2**, which appeared as an orange solid and, in the IR spectrum, exhibited at least three CO stretching bands (1973, 1956, and 1926 cm^{-1}). Its solid-state structure was unequivocally established by X-ray crystallography (Fig. 2), showing two molecules of **1** linked by $Co_2(CO)_6$ (Scheme 4). The geometry about the central cobalt atoms is trigonal bipyramidal, supported by a relatively large τ value of 0.84 (Table 2). The CO ligands attached to the terminal cobalt atoms are disordered, preventing a more in-depth structural analysis. Interestingly, the P–O bond of the appended phosphinite group contracts upon coordination to cobalt, and distance wise, it is almost indistinguishable from the P–O bonds within the pincer scaffold.

Most importantly, the ^{31}P{^{1}H} NMR spectrum of **2** confirms that this compound was the impurity found during our synthesis of {2,6-(^{i}Pr$_2$PO)$_2$-4-Me$_2$N-C$_6$H$_2$}Co(CO)$_2$. The proton NMR resonances of **2** are significantly broad, in contrast to the sharp C*H* and C*H*$_3$ resonances observed for the free ^{i}Pr$_2$PO group of **1**, which are also well separated from the resonances for the coordinated ^{i}Pr$_2$PO groups. Previous NMR studies of {2,6-(^{i}Pr$_2$PO)$_2$-4-R′-C$_6$H$_2$}Co(CO)$_2$[17] and {2,6-(^{i}Pr$_2$PO)$_2$-4-R′-C$_6$H$_2$}NiBr[24,32] have shown a strong correlation between the chemical shift value of the *ipso* carbon and the electronic property of the *para*-substituent. Specifically, introducing a more electron-withdrawing R′ group at the *para*-position results in the *ipso* carbon resonance being shifted more to the downfield region. Consistent with this analysis, upon coordination to cobalt, the appended ^{i}Pr$_2$PO group shifts the *ipso* carbon resonance from 128.46 ppm for **1** to 132.71 ppm for **2** (in CD$_2$Cl$_2$).[33] Other noticeable spectroscopic changes are for the *meta* and *para* carbons, which appear as a doublet of triplets and a doublet, respectively, in **1** but become two singlets in **2**.[34] These changes in splitting pattern are likely a reflection of the structural perturbation caused by the binding of the appended ^{i}Pr$_2$PO group to cobalt. In particular, three-bond carbon–phosphorus couplings are dependent on the torsion angles involved[35] and approximated by the Karplus equation.[36] Crystallographic data of **1** show P3–O3–C4–C$_{meta}$ torsion angles of 32.9(3)°, –149.13(16)°, –31.4(3)°, and 150.90(15)° for the two conformers (Fig. 1), although in solution, the C–O bond is expected to rotate freely. Coordination of the appended ^{i}Pr$_2$PO group is likely to restrict bond rotation, and according to the crystal structure of **2**, the P3–O3–C4–C$_{meta}$ torsion angles of –84.1(3)° and 102.2(3)° fall into the Karplus equation regime for a negligible coupling constant. Two-bond carbon–phosphorus couplings are much more complicated but known to be sensitive to conformation change.[37,38] It is worth noting that

Fig. 1. ORTEP drawings of $\{\kappa^P,\kappa^C,\kappa^P$-2,4,6-$(^iPr_2PO)_3C_6H_2\}Co(CO)_2$(1) at the 50% probability level (hydrogen atoms omitted for clarity). [Colour online.]

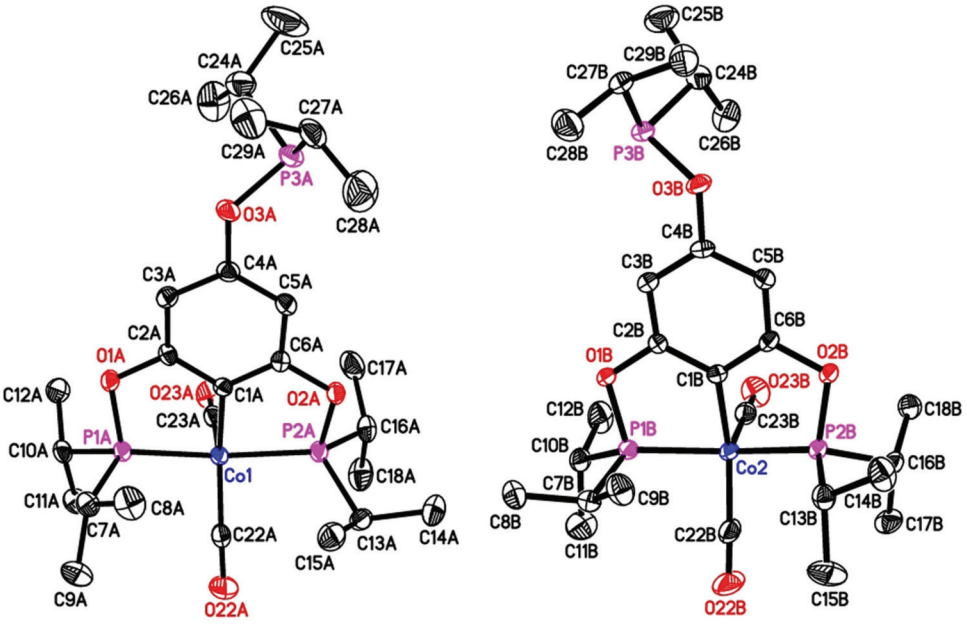

Table 2. Selected bond lengths (Å), angles (°), and geometry index for **1** and **2**.

	1 (molecule A)	**1** (molecule B)	**2**[a]
Co–C1	1.980(2)	1.971(2)	1.983(2)
Co–P1	2.1598(6)	2.1561(6)	2.1583(9)
Co–P2	2.1670(6)	2.1635(6)	2.1533(10)
Co–P3	N/A	N/A	2.1539(7)
Co–C22	1.750(2)	1.738(2)	1.854(6), 1.606(9)
Co–C23	1.789(2)	1.800(2)	1.678(6), 1.972(11)
C22–O22	1.152(3)	1.150(3)	1.147(6), 1.160(11)
C23–O23	1.140(3)	1.143(3)	1.145(7), 1.217(13)
P1–O1	1.6557(15)	1.6547(15)	1.6473(19)
P2–O2	1.6475(15)	1.6600(15)	1.638(2)
P3–O3	1.6755(15)	1.6780(15)	1.6426(18)
P1–Co–P2	152.09(2)	141.58(3)	155.62(4)
C1–Co–C22	145.50(10)	155.38(11)	126.8(2), 163.0(4)
C1–Co–C23	104.11(9)	97.87(9)	123.2(3), 98.6(4)
C22–Co–C23	110.38(11)	106.69(12)	109.9(3), 98.3(5)
P3–O3–C4	120.76(12)	121.07(13)	125.11(17)
τ^b	0.11	0.23	0.48, 0.12 (pincer); 0.84 (non-pincer)

[a]Because carbonyl groups attached to Co1 are disordered, two sets of data are provided for bonds and angles involving those carbonyl groups, as well as the geometry index. The numbers listed first are for Component A.

[b]$\tau = (\beta - \alpha)/60$; β and α are the two greatest bond angles (in degrees) about the cobalt.

the P3–O3–C4 angle expands from 120.76(12)° and 121.07(13)° in **1** to 125.11(17)° in **2**.

The method of activating the C–H bond of 1,3,5-$(^iPr_2PO)_3C_6H_3$ or a related triphosphinite can be extended to other transition metal systems for the synthesis of POCOP-type pincer complexes bearing an appended phosphinite group. A nickel complex **3** was readily prepared from 1,3,5-$(^iPr_2PO)_3C_6H_3$, $NiCl_2$, and 4-dimethylaminopyridine (Scheme 5), following a procedure similar to the one reported for the parent complex $\{2,6\text{-}(^iPr_2PO)_2C_6H_3\}NiCl$.[32] The product was characterized by NMR spectroscopy, X-ray crystallography (Fig. 3; Table 3), and elemental analysis. As expected, **3** (in C_6D_6) shows two distinctive phosphorus resonances: one at 187.28 ppm for the pincer part of the molecule and the other at 148.90 ppm for the dangling phosphinite.

Fig. 2. ORTEP drawing of $\{\kappa^P\text{-}\{\kappa^P,\kappa^C,\kappa^P$-2,4,6-$(^iPr_2PO)_3C_6H_2\}Co(CO)_2\}_2Co_2(CO)_6$(2) at the 50% probability level (hydrogen atoms omitted for clarity; carbonyl groups attached to Co1 and isopropyl groups attached to P2 are disordered, and they were refined using a two-component disorder model). [Colour online.]

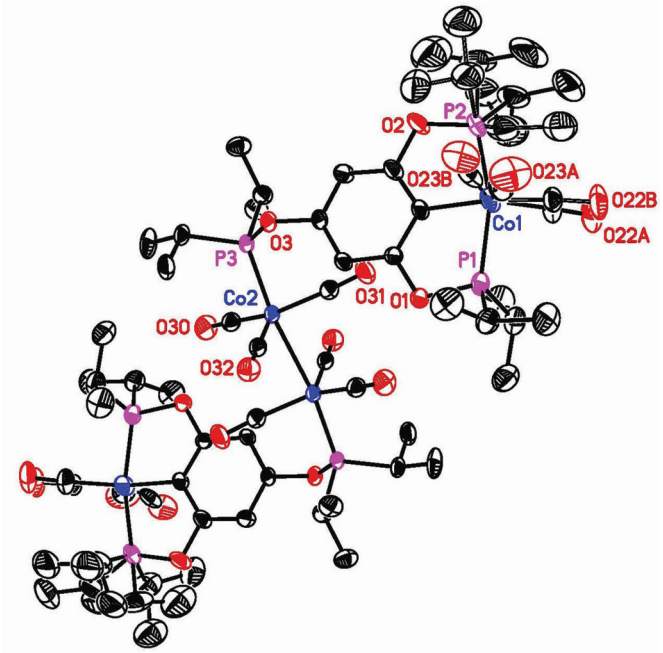

Conclusions

In this work, we have identified a tetranuclear species $\{\kappa^P\text{-}\{\kappa^P,\kappa^C,\kappa^P$-2,4,6-$(^iPr_2PO)_3C_6H_2\}Co(CO)_2\}_2Co_2(CO)_6$ as the impurity encountered during the synthesis of $\{2,6\text{-}(^iPr_2PO)_2\text{-}4\text{-}Me_2N\text{-}C_6H_2\}Co(CO)_2$. The presence of such an impurity is attributed to the incomplete monoamination of phloroglucinol with dimethylamine to form 5-(dimethylamino)resorcinol, which is a precursor to the pincer ligand 1,3-$(^iPr_2PO)_2$-5-Me_2N-C_6H_3. With the

Scheme 4. Reaction of $Co_2(CO)_8$ with 1 equiv. of 1,3,5-($^iPr_2PO)_3C_6H_3$.

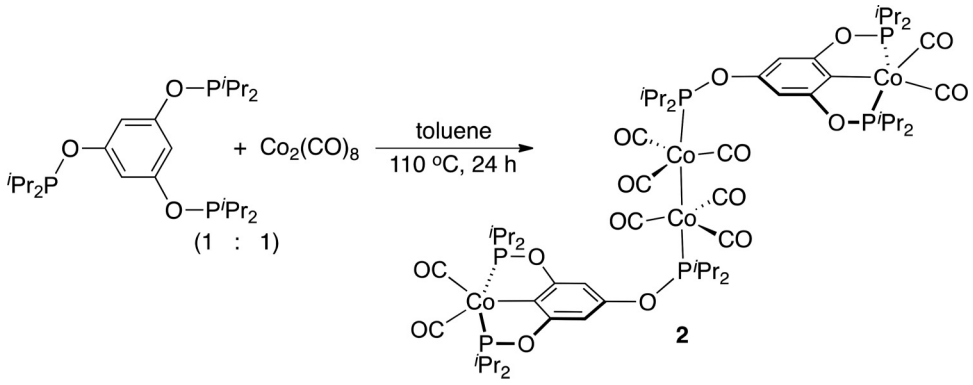

Scheme 5. Synthesis of a phosphinite-appended POCOP-type nickel pincer complex.

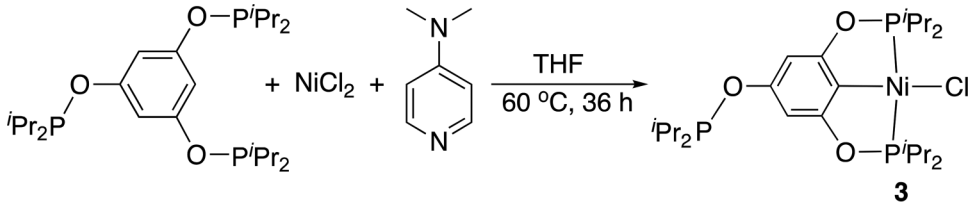

Fig. 3. ORTEP drawing of {$\kappa^P,\kappa^C,\kappa^P$-2,4,6-($^iPr_2PO)_3C_6H_2$}NiCl(3) at the 50% probability level (hydrogen atoms omitted for clarity). [Colour online.]

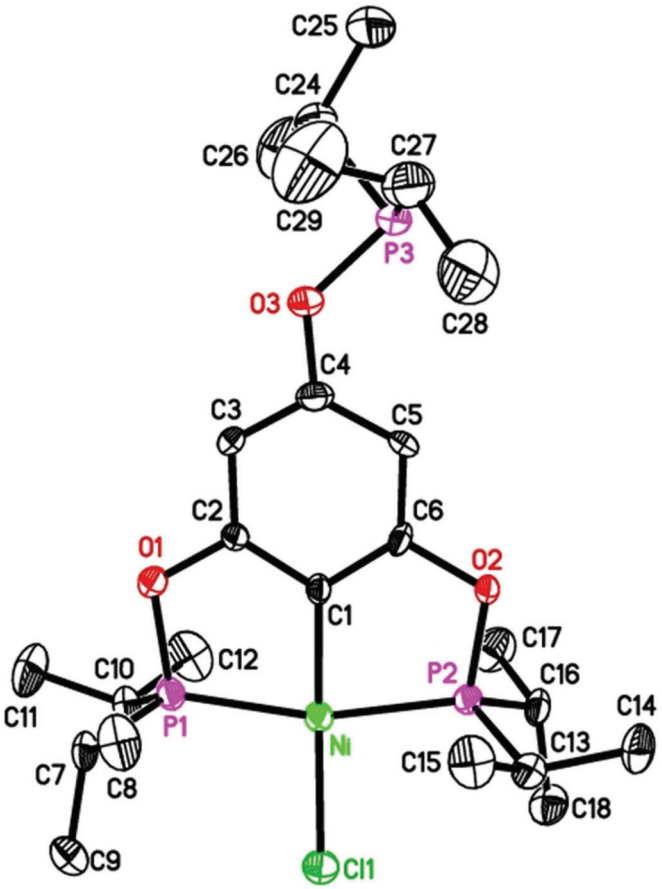

Table 3. Selected bond lengths (Å) and angles (°) for **3**.

Ni–C1	1.869(9)
Ni–P1	2.154(3)
Ni–P2	2.147(3)
Ni–Cl1	2.199(3)
P1–O1	1.649(7)
P2–O2	1.645(7)
P3–O3	1.655(8)
P1–Ni–P2	164.32(12)
C1–Ni–P1	82.6(3)
C1–Ni–P2	81.8(3)
C1–Ni–Cl1	177.0(3)
P3–O3–C4	125.9(7)

pre-synthesized 1,3,5-($^iPr_2PO)_3C_6H_3$, we have also demonstrated the possibility of activating its C–H bond with cobalt and nickel to yield phosphinite-appended pincer complexes {$\kappa^P,\kappa^C,\kappa^P$-2,4,6-($^iPr_2PO)_3C_6H_2$}Co(CO)$_2$ and {$\kappa^P,\kappa^C,\kappa^P$-2,4,6-($^iPr_2PO)_3C_6H_2$}NiCl. Molecules of this type have the potential to be implemented in catalyst immobilization, in gaining access to unique heterobimetallic complexes, and for late-stage modification of the pincer complexes.[27,39]

Supplementary data

NMR and IR spectra of the newly synthesized compounds and more detailed X-ray crystallographic information for **1–3** are available with the article through the journal Web site at http://nrcresearchpress.com/doi/suppl/10.1139/cjc-2020-0137. CCDC 1994013–1994015 contain the crystallographic data in CIF format for this paper. These data can be obtained, free of charge, via http://www.ccdc.cam.ac.uk/products/csd/request/ (or from the Cambridge Crystallographic Data Centre, 12 Union Road, Cambridge CB2 1EZ, U.K.; Fax: 44–1223–336033 or e-mail: deposit@ccdc.cam.ac.uk).

Acknowledgements

We thank the National Science Foundation (CHE-1800151) for support of this research. Crystallographic data were collected on a Bruker APEX-II CCD diffractometer (funded by NSF-MRI grant CHE–0215950), a Bruker Cu-IμS Photon-II diffractometer, or

through the SCrALS (Service Crystallography at Advanced Light Source) Program at Beamline 11.3.1 at the Advanced Light Source (ALS), Lawrence Berkeley National Laboratory (supported by the U.S. Department of Energy, Office of Energy Sciences Materials Sciences Division, under contract DE-AC02-05CH11231). JAK thanks Dr. Allen G. Oliver at the University of Notre Dame Molecular Structure Center for crystallographic data collection of **3** and helpful discussion regarding the twin refinement.

References

(1) Gómez-Benítez, V.; Baldovino-Pantaleón, O.; Herrera-Álvarez, C.; Toscano, R. A.; Morales-Morales, D. *Tetrahedron Lett.* **2006**, *47*, 5059. doi:10.1016/j.tetlet.2006.05.094.
(2) Morales-Morales, D. *Mini-Rev. Org. Chem.* **2008**, *5*, 141. doi:10.2174/157019308784223578.
(3) Choi, J.; MacArthur, A. H. R.; Brookhart, M.; Goldman, A. S. *Chem. Rev.* **2011**, *111*, 1761. doi:10.1021/cr1003503.
(4) Selander, N.; Szabó, K. J. *Chem. Rev.* **2011**, *111*, 2048. doi:10.1021/cr1002112.
(5) Haibach, M. C.; Kundu, S.; Brookhart, M.; Goldman, A. S. *Acc. Chem. Res.* **2012**, *45*, 947. doi:10.1021/ar3000713.
(6) Zargarian, D.; Castonguay, A.; Spasyuk, D. M. *Top. Organomet. Chem.* **2013**, *40*, 131. doi:10.1007/978-3-642-31081-2_5.
(7) Adhikary, A.; Guan, H. *ACS Catal.* **2015**, *5*, 6858. doi:10.1021/acscatal.5b01688.
(8) Murugesan, S.; Kirchner, K. *Dalton Trans.* **2016**, *45*, 416. doi:10.1039/C5DT03778F.
(9) Asay, M.; Morales-Morales, D. *Top. Organomet. Chem.* **2015**, *54*, 239. doi:10.1007/3418_2015_135.
(10) Kumar, A.; Bhatti, T. M.; Goldman, A. S. *Chem. Rev.* **2017**, *117*, 12357. doi:10.1021/acs.chemrev.7b00247.
(11) Morales-Morales, D., Editor. *Pincer compounds. Chemistry and applications*. Elsevier, Amsterdam, 2018.
(12) Albrecht, M.; van Koten, G. *Angew. Chem., Int. Ed.* **2001**, *40*, 3750. doi:10.1002/1521-3773(20011015)40:20<3750::AID-ANIE3750>3.0.CO;2-6.
(13) Molnár, Á.; Papp, A. *Coord. Chem. Rev.* **2017**, *349*, 1. doi:10.1016/j.ccr.2017.08.011.
(14) Huang, Z.; Brookhart, M.; Goldman, A. S.; Kundu, S.; Ray, A.; Scott, S. L.; Vicente, B. C. *Adv. Synth. Catal.* **2009**, *351*, 188. doi:10.1002/adsc.200800615.
(15) Vicente, B. C.; Huang, Z.; Brookhart, M.; Goldman, A. S.; Scott, S. L. *Dalton Trans.* **2011**, *40*, 4268. doi:10.1039/c0dt01369b.
(16) Sheludko, B.; Cunningham, M. T.; Goldman, A. S.; Celik, F. E. *ACS Catal.* **2018**, *8*, 7828. doi:10.1021/acscatal.8b01497.
(17) Li, Y.; Krause, J. A.; Guan, H. *Organometallics* **2018**, *37*, 2147. doi:10.1021/acs.organomet.8b00273.
(18) To remove phloroglucinol from 5-(dimethylamino)resorcinol, the ligand was dissolved in Et_2O, treated with a 1.0 mol/L HCl solution (~1.5 equiv.), and then extracted with water. The collected aqueous layer was neutralized with a 0.5 mol/L NaOH solution, and pure 5-(dimethylamino)resorcinol was obtained by extraction with Et_2O followed by evaporation under vacuum.
(19) Petrzilka, T.; Lusuardi, W. G. *Helv. Chim. Acta* **1973**, *56*, 510. doi:10.1002/hlca.19730560148.
(20) Lao, D. B.; Owens, A. C. E.; Heinekey, D. M.; Goldberg, K. I. *ACS Catal.* **2013**, *3*, 2391. doi:10.1021/cs400551g.
(21) Salem, H.; Ben-David, Y.; Shimon, L. J. W.; Milstein, D. *Organometallics* **2006**, *25*, 2292. doi:10.1021/om060005q.
(22) Bedford, R. B.; Betham, M.; Blake, M. E.; Coles, S. J.; Draper, S. M.; Hursthouse, M. B.; Scully, P. N. *Inorg. Chim. Acta* **2006**, *359*, 1870. doi:10.1016/j.ica.2005.07.050.
(23) Castonguay, A.; Spasyuk, D. M.; Madern, N.; Beauchamp, A. L.; Zargarian, D. *Organometallics* **2009**, *28*, 2134. doi:10.1021/om800840u.
(24) Vabre, B.; Spasyuk, D. M.; Zargarian, D. *Organometallics* **2012**, *31*, 8561. doi:10.1021/om3009475.
(25) Espinosa-Jalapa, N. Á.; Hernández-Ortega, S.; Le Goff, X.-F.; Morales-Morales, D.; Djukic, J.-P.; Le Lagadec, R. *Organometallics* **2013**, *32*, 2661. doi:10.1021/om400147x.
(26) Timpa, S. D.; Zhou, J.; Bhuvanesh, N.; Ozerov, O. V. *Organometallics* **2014**, *33*, 6210. doi:10.1021/om5008902.
(27) García-Eleno, M. A.; Padilla-Mata, E.; Estudiante-Negrete, F.; Pichal-Cerda, F.; Hernández-Ortega, S.; Toscano, R. A.; Morales-Morales, D. *New J. Chem.* **2015**, *39*, 3361. doi:10.1039/C5NJ00052A.
(28) Wellala, N. P. N.; Dong, H. T.; Krause, J. A.; Guan, H. *Organometallics* **2018**, *37*, 4031. doi:10.1021/acs.organomet.8b00619.
(29) Himmelbauer, D.; Stöger, B.; Veiros, L. F.; Pignitter, M.; Kirchner, K. *Organometallics* **2019**, *38*, 4669. doi:10.1021/acs.organomet.9b00651.
(30) The broadening is likely caused by the quadrupolar ^{59}Co nucleus.
(31) Addison, A. W.; Rao, T. N.; Reedijk, J.; van Rijn, J.; Verschoor, G. C. *J. Chem. Soc., Dalton Trans.* **1984**, 1349. doi:10.1039/DT9840001349.
(32) Pandarus, V.; Zargarian, D. *Organometallics* **2007**, *26*, 4321. doi:10.1021/om700400x.
(33) To avoid peak overlapping, CD_2Cl_2 was chosen as the preferred NMR solvent.
(34) When **2** was analyzed in C_6D_6, the resonance for the *meta* carbon was resolved as a triplet at 100.04 Hz ($J_{P\text{-}C}$ = 6.1 Hz) due to virtual coupling with P1 and P2.
(35) Murari, R.; Abd El-Rahman, M. M. A.; Wedmid, Y.; Parthasarathy, S.; Baumann, W. J. *J. Org. Chem.* **1982**, *47*, 2158. doi:10.1021/jo00132a034.
(36) Karplus, M. *J. Am. Chem. Soc.* **1963**, *85*, 2870. doi:10.1021/ja00901a059.
(37) Duddeck, H; Hanna, A. G. *Magn. Reson. Chem.* **1985**, *23*, 41. doi:10.1002/mrc.1260230112.
(38) Male, J. L.; Einstein, F. W. B.; Leong, W. K.; Pomeroy, R. K.; Tyler, D. R. *J. Organomet. Chem.* **1997**, *549*, 105. doi:10.1016/S0022-328X(97)00469-5.
(39) García-Eleno, M. A.; Quezada-Miriel, M.; Reyes-Martínez, R.; Hernández-Ortega, S.; Morales-Morales, D. *Acta Crystallogr. C Struct. Chem.* **2016**, *72*, 393. doi:10.1107/S2053229616005143.